PROCEEDINGS, 41st Workshop on Geothermal Reservoir Engineering
Stanford University, Stanford, California, February 22-24, 2016
SGP-TR-209

Reduced-Order Models to Predict Thermal Output for Enhanced Geothermal Systems

M. K. Mudunuru[1], S. Kelkar[1], S. Karra[1], D. R. Harp[1], G. D. Guthrie[1], and H. S. Viswanathan[1]

[1]Earth and Environmental Sciences Division, Los Alamos National Laboratory, Los Alamos, NM 87545, USA

maruti@lanl.gov

Keywords: enhanced geothermal systems, reduced-order models, thermal drawdown, data-limited problems.

ABSTRACT

Enhanced Geothermal Systems (EGS) present a significant and long-term opportunity for widespread power production from new geothermal sources. EGS approach makes it possible to tap otherwise inaccessible thermal resources in areas that lack traditional geothermal systems. It is estimated that within the USA alone the electricity production potential of EGS is in excess of 100GW. Hence, the efforts to accurately model and predict the performance of EGS reservoirs under various reservoir conditions (such as formation permeability, reservoir temperature, existing fracture/fault connectivity, and in-situ stress distribution) are vital. In this paper, we present a modeling study using data from the historic Fenton Hill Hot Dry Rock (HDR) project. This work is a part of a larger community-wide Geothermal Code Comparison effort, which is being supported by the US Department of Energy. The goal of our modeling study is to form Reduced-Order Models (ROMs) for fast model analysis and future predictions of thermal power output for an EGS reservoir. The ROMs will then be used to evaluate the influence of subsurface attributes, such as fracture zone permeability, bottom hole pressure, injection mass flow rate, and well factor on thermal power production curves.

1. INTRODUCTION AND MOTIVATION

Geomechanical models, rock mechanics models, and enhanced geothermal systems fall into the class of *data-limited problems*. This is because various rock properties form the basis for these models and it is extremely difficult to characterize them unambiguously (e.g., Starfield and Cundall (1988)). The U.S. Department of Energy Geothermal Technologies Office Code Comparison Study (GTO-CCS) has classified the problems arising in modeling EGS and other geological systems as *data-limited problems* (see White et al. (2015, 2016)) due to the paucity of available data and limited physical understanding of the underlying complex subsurface processes occurring in EGS reservoirs, see McClure and Horne (2014) and Kelkar et al. (2015). The purpose of modeling data-limited problems related to EGS is three-fold. The first objective is to develop efficient heat extraction technology from a variety of subsurface geothermal energy deposits in rock formations over a wide range of useful temperatures. Second objective is to evaluate the potential for thermal energy extraction at various stages in the development of prospective resources for commercial utilization. The final objective is to estimate and predict the lifetime of existing and potential EGS reservoirs on the basis of initial thermal energy extraction rate. In the next set of subsections, we give a brief description of the relevant GTO-CCS challenge problems, which are addressed in this paper. Complexity in modeling the underlying challenge problem and corresponding issues in tackling such data-limited problems are highlighted. From a practical point of view, we are interested in developing models to examine the potential for supplying thermal energy at sustained rates for commercial operations.

For the past few decades, different researchers have proposed a variety of modeling strategies to gain understanding and explore potential trade-offs and alternatives, rather than making absolute predictions of the thermal power output (which is the main objective of the underlying field-scale problem). The reason being that there is no collective agreement among field experts due to diverse perspectives. Robinson and Tester (1984), Barton and Zoback (1988), Grisby et al. (1989), Grisby and Tester (1989), Rodrigues et al. (1993), Kruger and Robinson (1994), Swenson et al. (1995), Roff et al. (1996), Fu et al. (2011), Ghassemi (2012), Kelkar et al. (2012), McClure and Horne (2014), Norbeck et al. (2014), Pandey et al. (2014, 2015), and Guo et al. (2016) are some of the popular modeling research efforts related to understanding EGS reservoirs. Each modeling approach provided a new understanding, interpretation, and insight into the complex processes taking place in various EGS reservoirs as each EGS reservoir is unique in its own perspective. For instance, see the discussion and review of ten historical EGS projects by McClure and Horne (2014). Herein, we shall a take a different route to model and understand the EGS systems based on model reduction. This methodology has proved quite successful in modeling and understanding other subsurface systems such as geologic carbon sequestration and petroleum reservoirs (see Cardoso et al. (2009), Pau et al. (2013), and Harp et al. (2016)). Subsection 1.2 discusses more on this aspect. Finally, subsection 1.3 provides the scope of the GTO-CCS challenge problem, study objectives, and outline of this paper.

1.1 Geothermal code comparison study: A brief description of the relevant challenge problem and field experiment

There are various challenge problems proposed by GTO-CCS. For a detailed description of the problem statements, field-scale data sets and relevant documents, see White and Phillips (2015) and White et al. (2015, 2016). Herein, we shall attempt to address one such challenge problem, wherein the aim is in predicting the thermal power output during the Long-Term Flow Test (LTFT) experiment of Phase II Reservoir at the Fenton Hill HDR test site, located near Los Alamos, New Mexico. This Phase II reservoir was designed to test the HDR concept at temperatures and thermal production rates near those required for a commercial electrical power plant.

Fenton Hill Phase II field activities started on April 3, 1979 with the drilling of well EE-2. On July 14, 1995, following an annular breakthrough in the injection well EE-3A, the reservoir circulation was discontinued. During this time, long-term circulating flow test was conducted. The operation of LTFT experiment at Fenton Hill lasted for 39 months with 11 months of active circulation through the reservoir. The Phase II reservoir comprised of a single injection well, EE-3A and single production well EE-2A. These wells are hydraulically connected via a complex joint network in otherwise impermeable hot rock. Tracer tests conducted during LTFT showed increasing mass flux in longer duration flow paths, indicating that flow was diverting away from shorter flow pathways thus reducing the possibility of short-circuiting of the fracture networks. The injection pressure was in the range of 25 MPa to 30 MPa and production backpressure ranged from 8 MPa to 13 MPa. The injection and production mass flow rates range from 7.5 [kg s^{-1}] to 8.5 [kg s^{-1}] and 5.5 [kg s^{-1}] to 7.0 [kg s^{-1}]. The injection and production temperatures at the well head ranged from 293.15 [K] to 303.15 [K] and 438.15 [K] to 458.15 [K]. Correspondingly, the bottomhole temperatures at the production well accounting for friction loss are between 453.15 [K] and 498.15 [K]. For more details on these data sets and other aspects (such as tracer data, microseismic data, fracture networks, fracture connectivity, injection and production wells entry points, and reactive-transport data), see Kelkar et al. (2015) and Brown et al. (2015).

According to Kelkar et al. (2015) and Brown et al. (2015), continuous long-term circulation periods were not fully achieved within the Phase II reservoir at Fenton Hill. Uncertainties remain about the thermal recovery performance of the reservoir over an extended period of time. Thus, the challenge problems proposed in GTO-CCS, seek solutions through numerical simulations that answer various questions concerning the performance of Phase II reservoir at Fenton Hill. Reservoir creation and simulation, fracture network connectivity, reactive and passive transport of tracers and chemical species, and thermal recovery/power production are the four major topical areas of interest for Code Comparison Studies. Numerical simulations and resulting solutions are to address the coupled nature of these aspects and demonstrate consistency with field-scale experimental observations made during the reservoir creation and circulation tests as a part of Phase II project at Fenton Hill. In this paper, we address the last aspect, which is the thermal recovery (or thermal power output) and compare it with the Phase II LTFT experiment.

1.2 Need for reduced-order models

In recent years, model reduction techniques have proven to be powerful tools for solving various problems in geosciences. In reservoir management and decision-making, ROMs are considered powerful techniques to address computational challenges associated with managing realistic reservoirs (see Alghareeb (2015)). Examples of some popular research and scientific endeavors on reduced-order modeling within the context of subsurface processes include Cardoso et al. (2009), Cardoso and Durlofsky (2010), He et al. (2011), Pau et al. (2013), and Pasetto et al. (2013). Loosely speaking, the problem of model reduction is to replace a given mathematical model of a complex system (or a set of processes) by a much “simpler” and “smaller” model than the original model while simulating essential aspects of the system. The resulting simpler and smaller model still describes, or atleast approximately describes, certain aspects of the system or the underlying process. There are several reasons why we need ROMs in the context of EGS. We provide two main and important reasons as follows:

- Inverse modeling, model calibration, optimal design, and parameter estimation involves repeated evaluation of forward models. These models can be computationally intensive and prohibitive for high-fidelity simulations and when there are complex underlying physical, chemical, and biological processes. Furthermore, comprehensive uncertainty quantification, sensitivity analysis, and parametric studies are needed to train physics-based or process-level models to accurately describe various subsurface processes. Reduced-order models and parametric reduced-order models can be used as numerical surrogates to circumvent such situations, thereby reducing the overall computational burden of these numerical simulations.

- In many-query applications such as EGS, a simple, efficient and predictive model is required for field use. Such a model can greatly reduce (or minimize) the associated operational costs, thereby maximizing the EGS power output potential.

1.3 Scope, study objectives, and outline of the paper

The scope and objective of the study is to develop ROMs for an EGS. Among the various outputs, which the ROMs produce, we are interested in thermal power produced. That is, we are interested in developing an efficient, predictive, and (possibly) simple reduced-order model for thermal power output. To achieve this the approach involves ROMs constructed using the results of complex 3D numerical simulations based on a massively parallel subsurface flow simulator PFLOTRAN (Lichtner et al. 2015) using Latin Hypercube Sampling (LHS) of the input parameters. The obtained ROMs are cross-validated against field-scale data sets and PFLOTRAN numerical simulations. Field-scale data sets (provided by the GTO-CCS) are based on the data extracted from Long Term Flow Test (LTFT) experiment from Fenton Hill HDR Phase-II reservoir. These data sets include injection pressure and production backpressures, injection and production flow rates, injection and production temperatures, and net thermal power extracted.

The paper is organized as follows: Section 2 describes the physics-based conceptual model, which approximately describes the Fenton Hill HDR Phase-II reservoir. It also provides a brief overview of the governing equations for fluid flow, thermal drawdown, and numerical methodology to solve the coupled conservation equations. Assumptions in modeling these systems are also outlined. In Section 2, we present numerical results for PFLOTRAN simulations based on Latin Hypercube Sampling of various inputs. From these numerical simulations, we estimate the material and system parameters, which are used in development of ROMs for thermal drawdown. Sensitivity analysis of the various input parameters is performed. From these sensitivity studies, key input parameters are identified for ROM construction. Workflow for ROM development is also described in this section. Section 3 details a procedure to construct reduced-order models for thermal power output. It also provides a brief overview of advanced model reduction methods and algorithms to construct ROMs for enhanced geothermal systems. Predictive capabilities of ROMs with respect to thermal power output, field-data, and PFLOTRAN numerical simulations are also discussed. Finally, conclusions are drawn in Section 4.

2. CONCEPTUAL MODEL, GOVERNING EQUATIONS, AND NUMERICAL METHODOLOGY

In this section, we briefly describe the governing equations for modeling physical processes involved in heat extraction within a jointed reservoir. We then present a physics-based conceptual model for an EGS reservoir and corresponding boundary conditions. Finally, we describe a numerical methodology to solve the system of coupled partial differential equations using the subsurface simulator PFLOTRAN. PFLOTRAN solves a system of nonlinear partial differential equations describing multiphase, multicomponent, and multiscale reactive flow and transport in porous materials. Here, we shall restrict to solving the governing equations resulting for fluid flow and heat transfer processes. Analyzing the geomechanics of the EGS and coupling with flow and reactive-transport is beyond the scope of the current study and will be part of our future work.

2.1 Governing equations: Fluid flow and heat transfer

In order to predict the heat extraction process, we solve the following set of governing equations. This includes balance of mass and balance of energy for fluid flow and thermal drawdown. The governing mass conservation equation for single phase saturated flow is given by:

$$\frac{\partial}{\partial t}(\varphi\rho) + \mathrm{div}[\rho\mathbf{q}] = Q_w \tag{1}$$

where φ is the porosity, ρ is the fluid density [kmol m^{-3}], $\mathbf{q}$ is the Darcy's flux [m s^{-1}], and Q_w is the volumetric source/sink term [kmol m^{-3} s^{-1}]. The Darcy's flux is given as follows:

$$\mathbf{q} = -\frac{k}{\mu}\mathrm{grad}[P - \rho g z] \tag{2}$$

where k is the intrinsic permeability [m^2], μ is the dynamic viscosity [Pa s], P is the pressure [Pa], g is the gravity [m s^{-2}], and z is the vertical component of the position vector [m]. The source/sink term is given as follows:

$$Q_w = \frac{\Gamma_{well} k}{\mu}\left(P - P_{bhp}\right)\delta\left(\boldsymbol{x} - \boldsymbol{x}_{ss}\right) \tag{3}$$

where Γ_{well} denotes the skin/well factor (which regulates the mass flow rate in the production well), $\boldsymbol{x}_{ss}$ denotes the location of the source/sink, P_{bhp} is the bottom hole pressure of the production well, and δ denotes the Dirac delta distribution. The governing equation for energy conservation to model thermal drawdown and corresponding heat extraction processes is given as follows:

$$\frac{\partial}{\partial t}\left(\varphi\rho U + (1 - \varphi)\rho_{rock} c_{p,rock} T\right) + \mathrm{div}\left[\rho\mathbf{q}H - \kappa\mathrm{grad}[T]\right] = Q_e \tag{4}$$

where U is the internal energy of the fluid, ρ_{rock} is the density of the porous rock, $c_{p,rock}$ is the heat capacity of the porous rock, T is the temperature of the fluid, H is the enthalpy of the fluid, κ is the thermal conductivity of porous rock, and Q_e is the source/sink term for heat extraction.

2.2 Physics-based conceptual model: EGS reservoir

Herein, we shall briefly describe a physics-based conceptual model used in the numerical simulation of phase-II Fenton Hill HDR reservoir. *It should be noted that this conceptual model is an approximation of a more complex system (see the reference by Kelkar et al. (2015) for a detailed description of the reservoir). Such an approximation is performed to understand the essential features and construct a model, which is amenable for numerical simulations*. Figure 1 provides a pictorial description of the reservoir. The reference datum, which is the reservoir top surface, is approximately located at a depth of 3000m. The dimensions and volume of the reservoir are taken to be equal to 1000 x 1000 x 1000 m^3. The fracture zone is an approximate representation of the region containing joint networks, whose dimensions are taken to be around 650 x 650 x 500 m^3. The fracture zone starting and ending coordinates are approximately taken to be (200m, 200m, 200m) and (850m, 850m, 700m). The injection and production wells are located at around (575m, 575m, 450m) and (675m, 500m, 625m). These are idealized as volumetric source/sink terms in performing the numerical simulations. Reservoir and fracture zone porosities are assumed to be equal to 0.0001 and 0.1. The reservoir rock density, rock specific heat capacity, rock thermal conductivity, rock permeability, fluid heat capacity, fluid density, and fluid injection temperature are taken as 2716 [kg m^{-3}], 803 [J kg^{-1} K^{-1}], 2.546 [W m^{-1} K^{-1}], 10^{-18} [m^2], 4187 [J kg^{-1} K^{-1}], 950 [kg m^{-3}], and 298.15 [K], (see Table 1 from reference Swenson et al. (1995)).

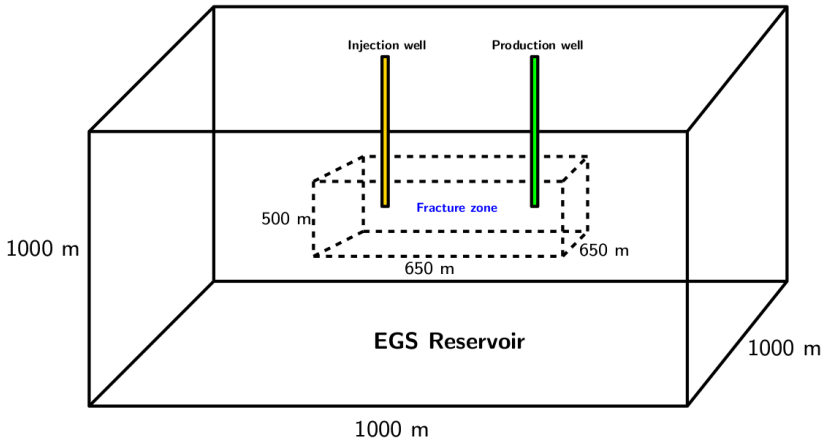

Figure 1: Physics-based conceptual model: EGS reservoir and fracture zone dimensions.

The reservoir/in-situ pressure is assumed to be around 13.2 [MPa] and temperature to be around 503.15 [K]. Zero gradient boundary conditions are assumed for solving heat transfer equations. Homogeneous Neumann (no-flux) boundary conditions are assumed for solving the flow equations. Figure 2 shows the respective injection pressure and production backpressure, injection and production mass flow rates, injection and production temperatures, and thermal power extracted during the Phase II LTFT experiment (which are provided by the GTO-CCS). These field-scale data sets are extracted from the Hot Dry Rock Final Report by Kelkar et al. (2015). The ranges for these values are used in constructing the Latin Hypercube Samples, which are then used in PFLOTRAN simulations to estimate the reservoir and other essential parameters. Details are discussed in the next subsection.

2.3 Numerical methodology

The governing flow and heat transfer equations are solved using PFLOTRAN simulator, which employs a fully implicit backward Euler for discretizing time and a two-point flux finite volume method for spatial discretization. The resulting non-linear algebraic equations are solved using a Newton-Krylov solver. From the numerical simulations based on Latin Hypercube Sampling for various input ranges using the field-scale data sets, we have the following parameters estimated to approximately fit thermal power production curve:

- Fracture zone permeability: 7.75 x 10^{-16} [m^2]
- Injection mass flow rate: 7.5 [kg s^{-1}]
- Production temperature: 438.15 [K]
- Bottom hole pressure: 9.5 [MPa]
- Skin/well factor to regulate mass flow rate in production well: 3.163 x 10^{-13}

The power output from the numerical simulation is calculated from the following expression:

Net power produced = (Production mass flow rate x Fluid heat capacity x Production temperature) – (Injection mass flow rate x Fluid heat capacity x Injection temperature)

Figure 3 shows the approximate fit of the numerical simulation with the field-scale data of the power output based on the parameters estimated. From this figure, it can inferred that the numerical simulation approximately describes the basic features of the power output profile during the LTFT experiment. Now using the above set of parameters, we perform sensitivity analysis to identify key sensitive input parameters for ROM construction. The next subsection describes the workflow for ROMs construction and corresponding sensitivity studies on various model parameters.

2.3 Sensitivity analysis, ROM development workflow, and numerical results

In this subsection, we perform sensitivity studies on various input/output model parameters to model EGS reservoirs. Such an analysis is performed to identify key sensitive parameters for ROM inputs. These model parameters include water injection rates and temperatures, reservoir/in-situ temperature, fracture zone permeability, length, width, and height of the reservoir, bottom hole pressure, well/skin factor, location of injection and production wells. Among these, sensitivity analysis based on PFLOTRAN numerical simulations suggested that mass flow rate at the injection well, skin/well factor to regulate mass flow rate in production well, fracture zone permeability, and bottom hole pressure are the key parameters.

Figure 4 shows the numerical simulation results for the above four key parameters. These figures are plotted for each sensitive parameter by keeping all other parameters fixed with respect to base case estimated values. For example, if fracture zone permeability is varied from the estimated value (which is equal 7.75 x 10^{-16} m^2), the other three estimated values for the parameters are kept constant. This is done to show, identify, and rank the key sensitive input parameters for the ROMs. Based on Figure 4, it is apparent that the power production is highly sensitive to varying fracture zone permeability and least sensitive to injection mass flow rates. Correspondingly, the skin/well factor to control mass flow rate in production well and bottom hole pressure (BHP) are second and third

in sensitivity ranks after fracture zone permeability. To consolidate, the ranking of importance of inputs for ROM development are given as follows (in the decreasing order):

1. Fracture zone permeability (power production varies in a non-linear fashion)
2. Skin/well factor to regulate mass flow rate in production well
3. Bottom hole pressure
4. Injection mass flow rate (power production varies in a linear fashion)

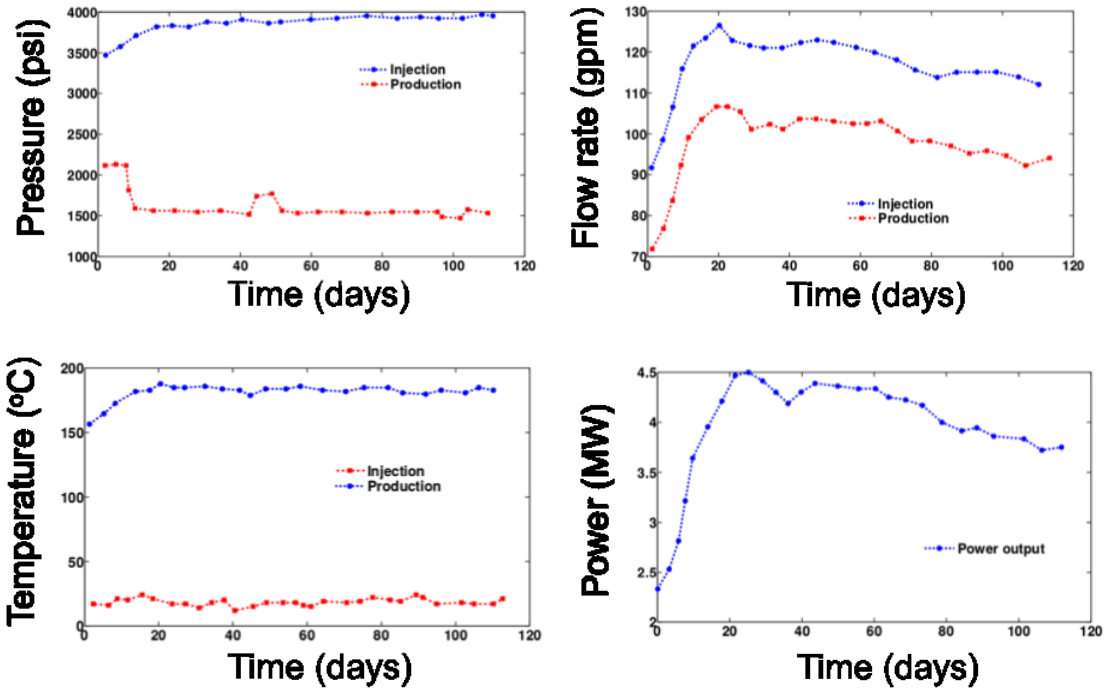

Figure 2: LTFT field-scale experiments of Fenton Hill phase-II reservoir: The top left figure shows the injection and production backpressures (psi) as a function of time (days). The injection backpressure ranges from 25MPa to 30MPa while the production backpressure ranges from 8MPa to 13 MPa. The top right figure shows the injection and production mass flow rates (gpm) as a function of time (days). The injection mass flow rate ranges from 7.5 [kg s^{-1}] to 8.5 [kg s^{-1}] while the production mass flow rate ranges from 5.5 [kg s^{-1}] to 7.0 [kg s^{-1}]. The bottom left figure shows the injection and production temperatures (^{o}C) vs time (days). The injection temperature ranges from 293.15 [K] to 303.15 [K] while the production temperature ranges from 438.15 [K] to 458.15 [K]. Correspondingly, accounting for wellbore friction losses, the bottomhole temperatures at the production well are between 453.15 [K] and 498.15 [K] (see subsection 3.15.1 in Kelkar et al. (2015)). The bottom right figure shows the thermal power output (MW) during the LTFT experiment.

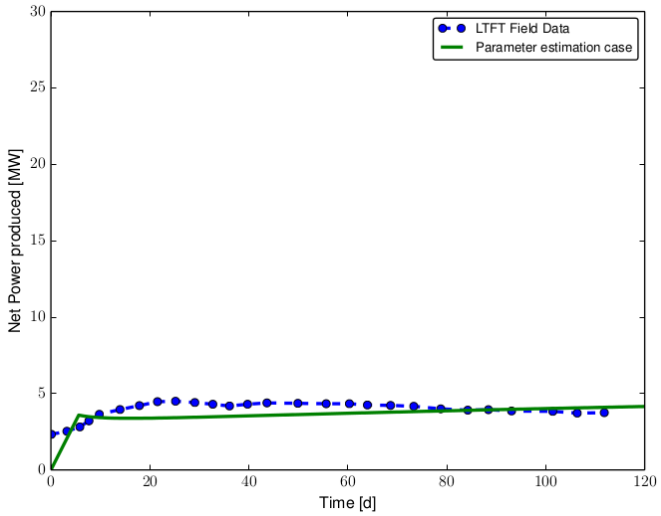

Figure 3: Comparison of thermal power output: LTFT experiment and parameter estimation case. The corresponding estimated parameters described in Subsection 2.3.

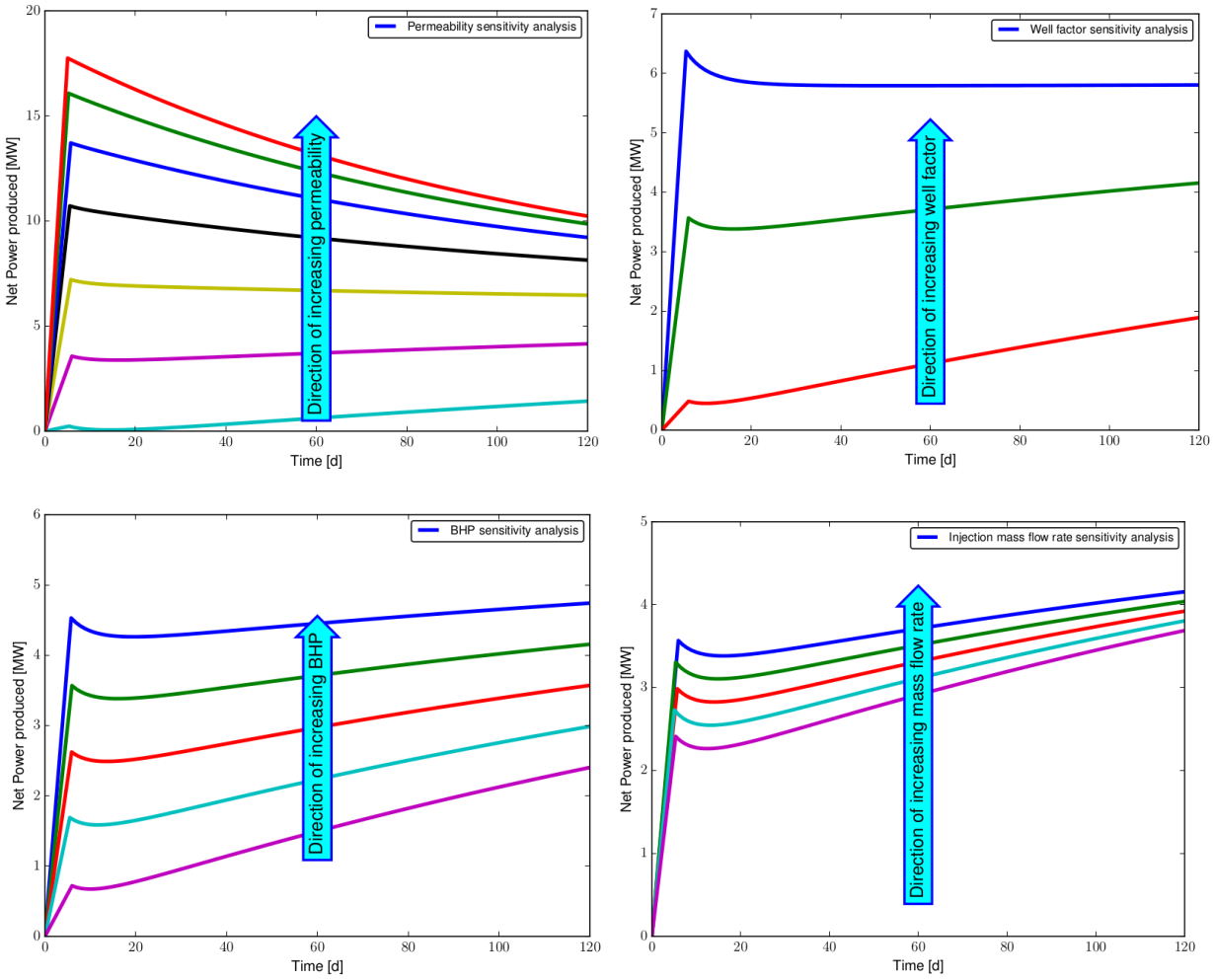

Figure 4: Sensitivity analysis for ROMs development: These figures show the sensitivity of thermal power production with respect to fracture zone permeability (top left figure), skin/well factor to regulate mass flow rate in the production well (top right figure), bottom hole pressure (bottom left figure), and injection mass flow rate (bottom right figure). The sensitivity analysis is performed by varying fracture zone permeability, well factor, bottom hole pressure, and injection mass flow rate within the range of 10^{-14} to 10^{-16} [m^2], 1.78 x 10^{-13} to 5.62 x 10^{-13}, 9.5 to 11 [MPa], and 7.5 to 8.5 [kg s^{-1}]. These values are constructed based on an educated guess of the fractured EGS system and considering the qualitative aspects of the field-scale data (see Section-3, Kelkar et al. (2015) for a detailed discussion on the qualitative & quantitative aspects of Fenton Hill phase-II reservoir and corresponding approximations).

The above aspects to obtain inputs for ROM development are summarized as a flowchart in Figure 5. This ROM development workflow is general for obtaining reduced-order models for *data-limited problems* such as enhanced geothermal systems, wherein it is not always possible to a priori simplify the model based on physical insight. In such cases, sensitivity analysis is performed to automatically identify potential simplifications. Designing such algorithms and workflows in essence, is the objective of the area of model order reduction. The next section describes an approach to construct ROMs for power output.

3. REDUCED-ORDER MODELLING

Reduced-order modeling is a promising approach, as many phenomena can be described well by a few dominated modes/mechanisms. The objective of model reduction methodologies is to use the knowledge generated by high fidelity and time-consuming numerical simulations to generate special functions that make use of properties of underlying systems, thereby obtaining a good understanding of the phenomena of interest. Subsection 1.1 discusses many reasons why such a detail is not needed. We shall now provide an overview of some popular model order reduction methods and algorithms. These techniques either use physical (or other) insight or sensitivity studies on model parameters as a basis to reduce the complexity of the underlying problem and obtain a good approximation of the required output in an efficient way.

Some popular model reduction methods include interpolation-based model order reduction, operational model order reduction, compact reduced-order modeling, truncated balanced realization, optimal Hankel-norm model order reduction, Gaussian process regression (GPR), proper orthogonal decomposition (POD), asymptotic waveform evaluation (AWE) and its variants, Pade via Lanczos (PVL) and its variants, spectral Lanczos decomposition method (SLDM), and truncation-based model order reduction. For more details on these methods, algorithms, and implementation aspects, see references Qu (2004), Schilders et al. (2008), and Quarteroni and Rozza (2014). *Here, we shall construct reduced-order models based on interpolation-based model order reduction methods, which result in simple thermal power output ROMs. These ROMs consist of a set of algebraic relations that depend on the key sensitive parameters that can be evaluated very quickly.*

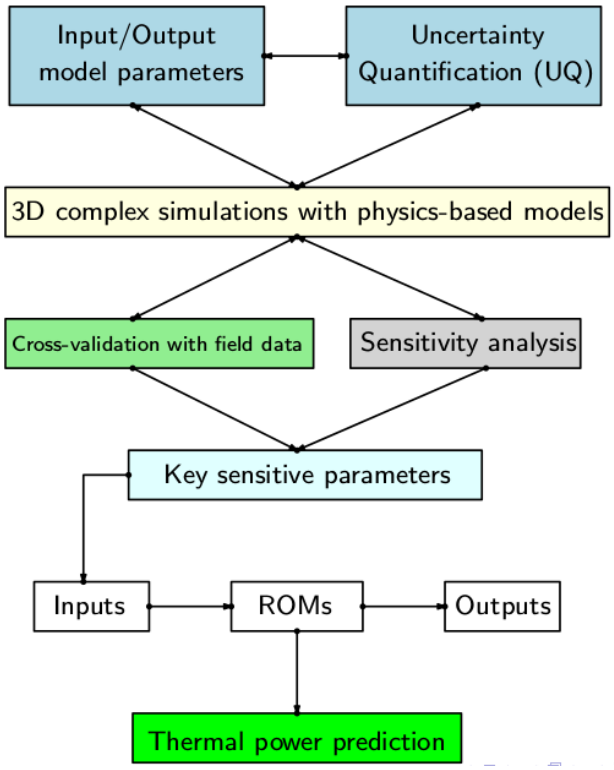

Figure 5: ROMs development flow diagram for EGS reservoir

3.1 Reduced-order models for power output based on interpolation-based methods

The reduced-order models are constructed using a combination of polynomials, trigonometric functions, exponentials, and smooth approximation of step functions. Logistic functions are chosen as the smooth-approximation of step functions. The rational behind choosing such functions are as follows: Polynomials, trigonometric functions, and exponentials capture the increase and decay part of the field-scale power output data and PFLOTRAN simulations, while the logistic functions are intended to capture the peaks and sudden variations. The coefficients of these functions are constructed through a non-linear least-squares regression fit to the PFLOTRAN simulations and using a small subset of field-scale data. To obtain the respective coefficients of the functions in the ROMs, the non-linear least-squares regression problem is solved using the optimization solvers available in the open-source Python package named Scipy (Jones et al. (2016)). Next, we propose and discuss three such reduced-order models. Each model has it own pros and cons, which are described below:

Thermal power output ROM-1:

$$Power_{rom-1} = a_0(t) + a_1(t)\left(\left|\log\left(k_{fz}\right)\right| + 10^{-6}t\right) + a_2(t)\left(\left|\log\left(k_{fz}\right)\right| + 10^{-6}t\right)^2 + a_3(t)\left(\left|\log\left(k_{fz}\right)\right| + 10^{-6}t\right)^3 \quad (5)$$

where t denotes the time in days, the coefficients a_0, a_1, a_2, a_3 are function of time [days], and k_{fz} is the fracture zone permeability [m^2]. These coefficients are given as follows:

$$
\begin{aligned}
a_0(t) &= -2.689 \square 10^3 - 9.951 \square 10^2 t + 28.37 t^2 - 3.013 \square 10^{-1} t^3 + 1.095 \square 10^{-3} t^4 \\
a_1(t) &= 5.517 \square 10^2 + 2.01 \square 10^2 t - 5.751 t^2 - 6.111 \square 10^{-2} t^3 - 2.222 \square 10^{-4} t^4 \\
a_2(t) &= -3.718 \square 10^1 - 1.347 \square 10^1 t + 3.867 \square 10^{-1} t^2 - 4.112 \square 10^{-3} t^3 + 1.495 \square 10^{-5} t^4 \\
a_3(t) &= 8.241 \square 10^3 + 2.998 \square 10^{-1} t - 8.634 \square 10^{-3} t^2 + 9.184 \square 10^{-5} t^3 - 3.339 \square 10^{-7} t^4
\end{aligned}
\tag{6}
$$

Thermal power output ROM-2:

$$
\begin{aligned}
Power_{rom-2} = b_0(t) + b_1(t)\left(\left|\log\left(k_{fz}\right)\right| + 10^{-6} t\right) + b_2(t)\left(\left|\log\left(k_{fz}\right)\right| + 10^{-6} t\right)^2 + b_3(t)\left(\left|\log\left(k_{fz}\right)\right| + 10^{-6} t\right)^3 + \\
\underbrace{\sum_{i=1}^{29} m_i \left(1 + \tanh\left(n_i\left(t - t_i\right)\right)\right)^{r_i}}_{Smooth\ approximation\ of\ Heaviside\ function}
\end{aligned}
\tag{7}
$$

where the coefficients b_0, b_1, b_2, b_3 are function of time [days], which are given as follows:

$$
\begin{aligned}
b_0(t) &= 2.318 \square 10^3 - 2.466 \square 10^3 t + 1.338 \square 10^2 t^2 - 3.413 t^3 + 4.612 \square 10^{-2} t^4 \\
&\quad - 3.393 \square 10^{-4} t^5 + 1.376 \square 10^{-6} t^6 - 3.538 \square 10^{-9} t^7 + 6.869 \square 10^{-12} t^8 \\
&\quad - 2.307 \square 10^3 \left(0.1\right)^t + 1.342 \sin(t) \\
b_1(t) &= -4.623 \square 10^2 + 4.992 \square 10^2 t - 2.713 \square 10^1 t^2 + 6.918 \square 10^{-1} t^3 - 9.339 \square 10^{-3} t^4 \\
&\quad + 6.856 \square 10^{-5} t^5 - 2.766 \square 10^{-7} t^6 + 7.056 \square 10^{-10} t^7 - 1.369 \square 10^{-12} t^8 \\
&\quad - 2.307 \square 10^3 \left(0.1\right)^t - 2.676 \square 10^{-1} \sin(t) \\
b_2(t) &= 3.103 \square 10^1 - 3.353 \square 10^1 t + 1.825 t^2 - 4.652 \square 10^{-2} t^3 + 6.28 \square 10^{-4} t^4 \\
&\quad - 4.608 \square 10^{-6} t^5 + 1.858 \square 10^{-8} t^6 - 4.734 \square 10^{-11} t^7 + 9.191 \square 10^{-14} t^8 \\
&\quad - 3.087 \square 10^1 \left(0.1\right)^t + 1.796 \square 10^{-2} \sin(t) \\
b_3(t) &= -6.997 \square 10^{-1} + 7.477 \square 10^{-1} t - 4.073 \square 10^{-2} t^2 + 1.038 \square 10^{-3} t^3 - 1.402 \square 10^{-5} t^4 \\
&\quad + 1.031 \square 10^{-7} t^5 - 4.168 \square 10^{-10} t^6 - 1.068 \square 10^{-12} t^7 - 2.073 \square 10^{-15} t^8 \\
&\quad + 6.964 \square 10^{-1} \left(0.1\right)^t - 4.048 \square 10^{-4} \sin(t)
\end{aligned}
\tag{8}
$$

The parameters t_i [days] are chosen in such a way that the ROM outputs be close to that of the field-scale LTFT thermal power output at these i^{th} time-snapshots/time-levels. *Note that these values are not arbitrary. They correspond to the discrete-time levels with respect to discrete thermal power outputs extracted from the field-scale LTFT thermal power data obtained from the GTO code comparison project.* These values are given as follows:

$$
\begin{aligned}
&t_1 = 10,\ t_2 = 15,\ t_3 = 17.5,\ t_4 = 19,\ t_5 = 20,\ t_6 = 21,\ t_7 = 22.5,\ t_8 = 25,\ t_9 = 30,\ t_{10} = 32.5 \\
&t_{11} = 35,\ t_{12} = 37.5,\ t_{13} = 50,\ t_{14} = 52.5,\ t_{15} = 55,\ t_{16} = 60,\ t_{17} = 62.5,\ t_{18} = 65,\ t_{19} = 70,\ t_{20} = 75 \\
&t_{21} = 80,\ t_{22} = 85,\ t_{23} = 87.5,\ t_{24} = 90,\ t_{25} = 95,\ t_{26} = 100,\ t_{27} = 105,\ t_{28} = 110,\ t_{29} = 112.5
\end{aligned}
\tag{9}
$$

The coefficients m_i, n_i, r_i are given as follows:

$$
\begin{aligned}
&m_1 = 0.1,\ m_2 = 0.085,\ m_3 = 0.05,\ m_4 = -0.0125,\ m_5 = 0.125,\ m_6 = 0.1,\ m_7 = -0.0125,\\
&m_8 = 0.085,\ m_9 = -0.075,\ m_{10} = -0.085,\ m_{11} = 0.085,\ m_{12} = 0.125,\ m_{13} = -0.085,\\
&m_{14} = -0.01,\ m_{15} = -0.05,\ m_{16} = -0.075,\ m_{17} = -0.075,\ m_{18} = -0.025,\ m_{19} = -0.015,\\
&m_{20} = -0.15,\ m_{21} = -0.05,\ m_{22} = -0.05,\ m_{23} = -0.05,\ m_{24} = -0.15,\ m_{25} = -0.1,\\
&m_{26} = -0.085,\ m_{27} = -0.175,\ m_{28} = -0.05,\ m_{29} = 0.05
\end{aligned}
\tag{10}
$$

$$
n_1 = n_2 = n_3 = 100;\ n_4 \text{ to } n_{29} = 1000 \tag{11}
$$

$$
\begin{aligned}
&r_1 = 1,\ r_2 = 1,\ r_3 = 1,\ r_4 = 0.5,\ r_5 = 0.25,\ r_6 = 0.5,\ r_7 = 0.1,\ r_8 = 0.25,\ r_9 = 0.75,\ r_{10} = 0.02\\
&r_{11} = 0.01,\ r_{12} = 0.01,\ r_{13} = 0.25,\ r_{14} = 1.5,\ r_{15} = 1.75,\ r_{16} = r_{17} = r_{18} = r_{19} = r_{20} = 0.01\\
&r_{21} = r_{22} = r_{23} = 0.01,\ r_{24} = 0.025,\ r_{25} = 0.075,\ r_{26} = 0.01,\ r_{27} = 0.15,\ r_{28} = 0.01,\ r_{29} = 0.01
\end{aligned}
\tag{12}
$$

Thermal power output ROM-3:

$$
Power_{rom-3} = c_0(t) + c_1(t)\left(\left|\log\left(k_{fz}\right)\right| + 10^{-6}t\right) + c_2(t)\left(\left|\log\left(k_{fz}\right)\right| + 10^{-6}t\right)^2 + c_3(t)\left(\left|\log\left(k_{fz}\right)\right| + 10^{-6}t\right)^3 \tag{13}
$$

where the coefficients c_0, c_1, c_2, c_3 are function of time [days]. These are given as follows:

$$
\begin{aligned}
c_0(t) &= 7.913\square 10^2 - 1.747\square 10^3 t + 2.089\square 10^1 t^2 + 5.173t^3 - 3.234\square 10^{-1}t^4\\
&\quad + 9.397\square 10^{-3}t^5 - 1.613\square 10^{-4}t^6 + 1.727\square 10^{-6}t^7 - 1.134\square 10^{-8}t^8\\
&\quad + 4.183\square 10^{-11}t^9 - 6.627\square 10^{-14}t^{10}\\
c_1(t) &= -1.578\square 10^2 + 3.557\square 10^2 t - 4.613t^2 - 1.019t^3 + 6.432\square 10^{-2}t^4\\
&\quad - 1.872\square 10^{-3}t^5 + 3.215\square 10^{-5}t^6 - 3.442\square 10^{-7}t^7 + 2.261\square 10^{-9}t^8\\
&\quad - 8.337\square 10^{-12}t^9 + 1.321\square 10^{-14}t^{10}\\
c_2(t) &= 1.059\square 10^1 - 2.391\square 10^1 t + 3.136\square 10^{-1}t^2 + 6.835\square 10^{-2}t^3 - 4.316\square 10^{-3}t^4\\
&\quad + 1.256\square 10^{-4}t^5 - 2.158\square 10^{-6}t^6 + 2.311\square 10^{-8}t^7 - 1.517\square 10^{-10}t^8\\
&\quad + 5.597\square 10^{-13}t^9 - 8.868\square 10^{-16}t^{10}\\
c_3(t) &= -2.388\square 10^{-1} + 5.305\square 10^{-1}t - 6.637\square 10^{-3}t^2 - 1.553\square 10^{-3}t^3 + 9.754\square 10^{-5}t^4\\
&\quad - 2.837\square 10^{-6}t^5 + 4.871\square 10^{-8}t^6 - 5.215\square 10^{-10}t^7 + 3.425\square 10^{-12}t^8\\
&\quad - 1.263\square 10^{-14}t^9 + 2.001\square 10^{-17}t^{10}
\end{aligned}
\tag{14}
$$

3.2 Discussion and inferences: Predictive capabilities of ROMs with respect to field-scale data and PFLOTRAN simulations

We shall now provide a rationale behind the construction of these ROMs. Moreover, we shall analyze the capabilities of these three reduced-order models in describing the trends in field-scale data and PFLOTRAN simulations. The motivation behind the construction of ROM-1 is simplicity. This reduced-order model consists of power-series terms (up to order four) involving natural logarithm of fracture zone permeability and time. The coefficients of the ROM-1 are constructed by matching the power output of PFLOTRAN numerical simulations at certain fixed intervals of time (for various fracture zone permeabilities). Figure 6 shows the predictions of ROM with respect to numerical simulations and the LTFT experiment. From this figure, qualitatively and quantitatively, it is evident that ROM-1 is able to accurately describe the power output of numerical simulations for low values of fracture zone permeability. However, as the fracture zone permeability increases, there is a considerable deviation between ROM-1 outputs and PFLOTRAN numerical simulations. This is because ROM-1 is constructed by matching PFLOTRAN numerical simulations only at certain time intervals. Moreover, the polynomial order considered to construct the reduced-order model is very low.

In case of predicting the field-scale data, ROM-1 is able to describe only certain essential features of the field-scale data. These aspects include the initial increase of power output, the corresponding decrease after the time *t = 20 days, and* then an increase in the power output after *t = 100 days*. However, quantitatively, the difference in power output values of ROM-1 and LTFT experiment are

considerably high. This formed the motivation to construct ROM-2. From equations (7)-(12), it is evident that ROM-2 is a complex model. The motivation behind the construction of such a complex model is that we would like to accurately describe the LTFT experiment at various time intervals. The ROM-2 is constructed by adding smooth approximations of step functions and higher-order polynomials to ROM-1. *These time intervals are chosen based on the data extracted from the documents provided by the geothermal code comparison project. That is, at these time levels power output is known*. The smooth approximations of step functions are chosen at these points to match the power output of LTFT experiment. Figure 7 shows the comparison of ROM-2 output with respect to PFLOTRAN numerical simulations and LTFT experiment. From this figure, it evident that ROM-2 power output closely matches the LTFT experiment, qualitatively and quantitatively. However, ROM-2 over predicts the numerical simulations, quantitatively. Qualitatively, the trend is similar to ROM-1 and captures the essential aspects of the numerical simulations even for high permeabilities.

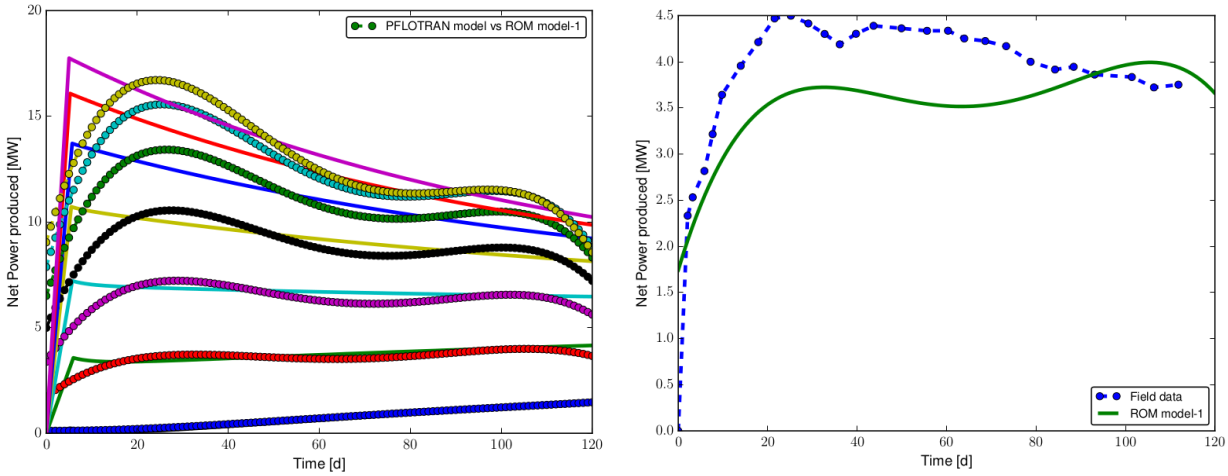

Figure 6: Thermal power output ROM-1: The left figure compares the ROM-1 output with respect to PFLOTRAN numerical simulations. The right figure compares the predictions of ROM-1 with respect to LTFT field-scale power output data set during phase-II experiment.

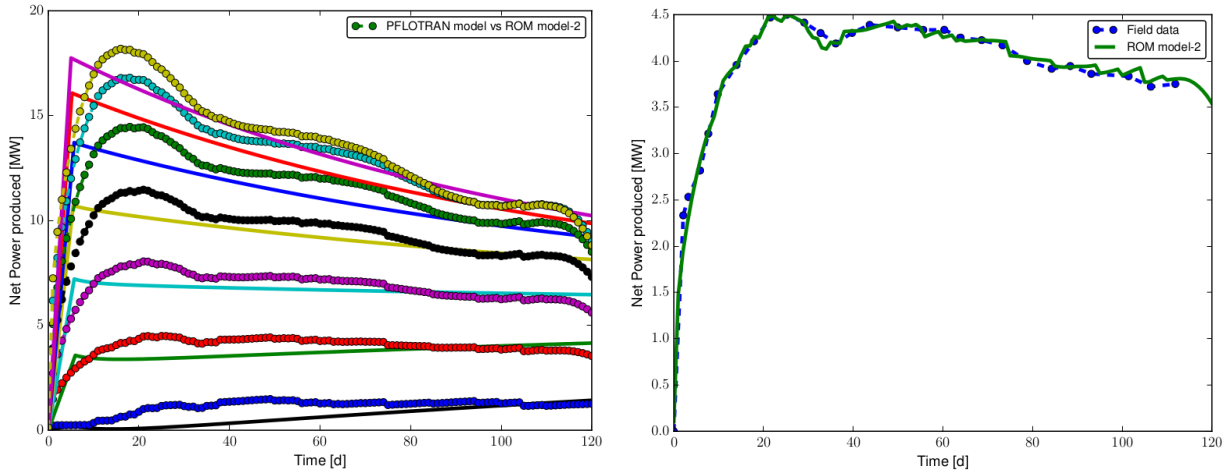

Figure 7: Thermal power output ROM-2: The left figure compares the ROM-2 output with respect to PFLOTRAN numerical simulations. The right figure compares the predictions of ROM-2 with respect to LTFT field-scale power output data set during phase-II experiment.

Motivated by these two ROMs, ROM-3 is constructed. The philosophy of ROM-3 is to use only polynomials. The number of terms is determined by the coefficient values. The maximum possible order for the polynomial chosen is 10. This is because as the order of polynomial increases the values of the coefficient are close to machine precision (close to zero). Figure 8 shows the thermal power output of ROM-3 as compared to numerical simulations and LTFT experiment. From this figure, it is apparent that the ROM-3 is accurately able to describe the trend in the behavior of thermal power output. For numerical simulations, as the permeability increases the deviations in the output values of ROM-3 and PFLOTRAN numerical simulations are not very large as compared to ROM-1 and ROM-2. In case of LTFT experiment, ROM-3 is able to accurately describe the increase in the thermal power output in initial stages. After time $t = 20$ days, when compared to the performance of ROM-2, ROM-3 is not exactly a close match to the LTFT data quantitatively. However, qualitatively, ROM-3 is a much better model compared to ROM-1 due to the incorporation of higher-order polynomials. In short, ROM-3 neither overfits nor underfits the LTFT experiment data. Hence, ROM-3 is a better model compared to

ROM-2 and ROM-1. The model can be improved by incorporating other input terms such as well factor, bottom hole pressure, and injection mass flow rates. This is beyond the scope of the current paper and will be considered in our future work.

4. CONCLUDING REMARKS AND FUTURE WORK

In this paper, we have presented various reduced-order models to describe different aspects of the numerical simulations and LTFT field-scale power output data of phase-II Fenton hill geothermal reservoir. First, we described the governing equations for fluid flow in the fractured reservoir and corresponding thermal drawdown. Second, we have presented a physics-based conceptual model for an EGS reservoir. The conceptual model is an approximation of a more complex system, which is performed to understand the essential features of the systems and make it amenable for numerical simulations. Field-scale data sets, which are extracted from the documents provided by the geothermal code comparison project, are used to estimate the parameters of the EGS system under consideration. These data sets include backpressures, mass flow rates, and temperatures at both injection and production sites. Third, sensitivity analysis is performed on these inputs to identify and rank the key parameters. These key parameters, which are the outcome of the sensitivity analysis is used as inputs for ROMs development. Finally, the ROMs are developed using the numerical simulations obtained based on Latin Hypercube Sampling of the input data. We proposed three different ROMs, each describing key and essential features of the LTFT power output data. The first ROM is a simple model and is able to accurately describe the power output at low fracture zone permeabilities. The second ROM is a complex model and is able to closely match the LTFT power output data. However, the second ROM considerably deviates from the PFLOTRAN numerical simulations for large values of fracture zone permeabilities. The third ROM is constructed by taking the best aspects of ROM-1 and ROM-2. ROM-3 is able to quantitatively and qualitatively describe the trend in the power output at different time levels for both PFLOTRAN numerical simulations and LTFT power output data. From these ROM development workflows and sensitivity analyses, it is evident that this study has demonstrated that simple reduced-order models are able to capture various complex features in the system. This work provides confidence in developing simple and efficient reduced-order models for field use.

4.1 Future work

In this paper, the ROMs are developed based on the most important parameter, which is the fracture zone permeability. However, from the sensitivity analysis it is evident that well factor, bottom hole pressure, and injection mass flow rate also play an important role in power output predictions. So based on these aspects, we describe the workflow of our future work. These are given as follows:

1. To construct ROMs that takes into account all the other three sensitive parameters in addition to fracture zone permeability.

2. To obtain an estimate or *predict the range of the thermal power production* using the constructed ROMs for a duration of 5, 10, 15, and 20 years beyond the LTFT.

3. Training the proposed system-level models and to compare the predictive capabilities of the proposed ROMs with respect to Phase I Fenton Hill HDR reservoir and for future EGS reservoirs. This will provide confidence in the proposed ROMs and system-level models in predicting power output for various other EGS reservoirs.

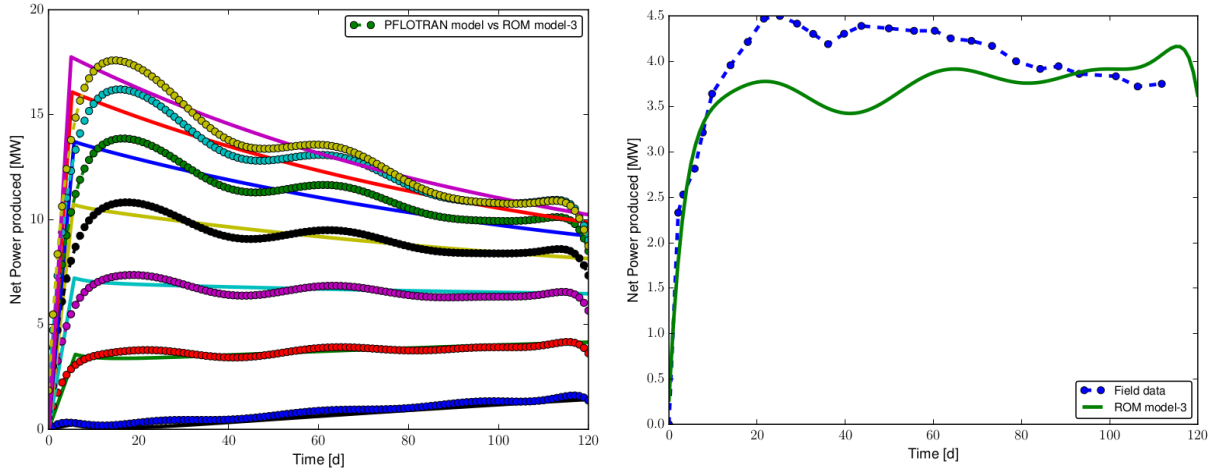

Figure 8: Thermal power output ROM-3: The left figure compares the ROM-3 output with respect to PFLOTRAN numerical simulations. The right figure compares the predictions of ROM-3 with respect to LTFT field-scale power output data during the phase-II experiment.

ACKNOWLEDGMENTS

This work is supported by the U.S. Department of Energy (DOE) - Geothermal Technologies Program (GTO) Office under contract DE-AC52-06NA25396. MKM thanks Don Brown for many useful and knowledgeable discussions.

REFERENCES

Alghareeb, Z.M.: Optimal Reservoir Management Using Adaptive Reduced-Order Models, PhD Dissertation, Massachusetts Institute of Technology, (2015).

Brown, D.W., Duchane, D.V., Heiken, G., and Hriscu, V.T.: Mining the Earth's Heat: Hot Dry Rock Geothermal Energy, *Springer*, (2012).

Barton, C.A, and Zoback, M.D.: In-situ Stress Orientation and Magnitude at the Fenton Geothermal Site, New Mexico, Determined From Wellbore Breakouts, *Geophysical Research Letters*, **15**, (1988), 467-470.

Cardoso, M.A., Durlofsky, L.J., and Sarma, P.: Development and Application of Reduced-Order Modeling Procedures for Subsurface Flow Simulation, *International Journal for Numerical Methods in Engineering*, **77**, (2009), 1322-1350.

Cardoso, M.A., and Durlofsky, L.J.: Linearized Reduced-Order Models for Subsurface Flow Simulations, *Journal of Computational Physics*, **229**, (2010), 681-700.

Dreesen, D., Malzahn, M., Fehler, M., and Dash, Z.: Identification of MHF Fracture Planes and Flow Paths: A Correlation of Well Log Data with Patterns in Locations of Induced Seismicity, LA-UR-87-2082, July 1987.

Fu, P., Johnson, S.M., Hao, Y., and Carrigan, C.R.: Fully Coupled Geomechanics and Discrete Flow Network Modeling of Hydraulic Fracturing for Geothermal Applications, *Proceedings*, 36th Stanford Geothermal Workshop, Stanford University, Stanford, CA, (2011).

Ghassemi, A.: A Review of Some Rock Mechanics Issues in Geothermal Reservoir Development, *Geotechnical and Geological Engineering*, **30**, (2012), 647-664.

Grisby, C.O., Tester, J.W., Trujillo Jr., P.E., and Counce, D.A.: Rock-Water Interactions in the Fenton-Hill, New Mexico, Hot Dry Rock Geothermal Systems-I. Fluid Mixing and Chemical Geothermometry, *Geothermics*, **18**, (1989), 629-656.

Grisby, C.O., Tester, J.W., Trujillo Jr., P.E., and Counce, D.A.: Rock-Water Interactions in the Fenton-Hill, New Mexico, Hot Dry Rock Geothermal Systems-II. Modeling Geochemical Behavior, *Geothermics*, **18**, (1989), 657-676.

Guo, B., Fu, P., Hao, Y., Peters, C.A., and Carrigan, C.R.: Thermal Drawdown-Induced Flow Channeling in a Single Fracture in EGS, *Geothermics*, **61**, (2016), 46-62.

Harp, D.R., Pawar, R., Carey, J.W., and Gable, C.W.: Reduced Order Models of Transient CO_2 and Brine Leakage along Abandoned Wellbores from Geologic Carbon Sequestration Reservoirs, *International Journal of Greenhouse Gas Control*, **45**, (2016), 150-162.

He, J., Saetrom, J., and Durlofsky, L.J.: Enhanced Linearized Reduced-Order Models for Subsurface Flow Simulation, *Journal of Computational Physics*, **230**, (2011), 8313-8341.

Jones, E., Oliphant, T., Peterson, P., and others: SciPy: Open Source Scientific Tools for Python, http://www.scipy.org/, (2016).

Kelkar, S., Lewis, K., Hickman, S., Davatzes, N.C., Moss, D., and Zyvoloski, G.: Modeling Coupled Thermal-Hydrological-Mechanical Processes During Shear Simulation of an EGS Well, *Proceedings*, 37th Stanford Geothermal Workshop, Stanford University, Stanford, CA, (2012).

Kelkar, S., WoldeGabriel, G., and Rehfeldt, K.: Hot Dry Rock Final Report, Geothermal Energy Development at Los Alamos National Laboratory: 1970-1995, LA-UR-15-22668, April 2015.

Kelkar, S., WoldeGabriel, G., and Rehfeldt, K.: Lessons Learned from the Pioneering Hot Dry Rock Project at Fenton Hill, USA, *Geothermics*, DOI:10.1016/j.geothermics.2015.08.008, (2015).

Kruger, P., and Robinson, B.: Heat Extracted From the Long Term Flow Test in the Fenton Hill HDR Reservoir, *Proceedings*, 19th Stanford Geothermal Workshop, Stanford University, Stanford, CA, (1994).

Lichtner, P.C., Hammond, G.E., Lu, C., Karra, S., Bisht, G., Andre, B., Mills, R.T., and Kumar, J.: PFLOTRAN User Manual: A Massively Parallel Reactive Flow and Transport Model for Describing Surface and Subsurface Processes, Technical Report No.: LA-UR-15-20403, Los Alamos National Laboratory, (2015).

McClure, M.W., and Horne, R.N.: An investigation of simulation mechanisms in Enhance Geothermal System, *International Journal of Rock Mechanics & Mining Sciences*, **72**, (2014), 242-260.

Norbeck, J., Huang, H., Podgorney, R., and Horne, R.: An Integrated Discrete Fracture Model for Description of Dynamic Behavior in Fractured Reservoirs, *Proceedings*, 39th Stanford Geothermal Workshop, Stanford University, Stanford, CA, (2014).

Pandey, S.N., Chaudhuri, A., Kelkar, S., Sandeep, V.R., and Rajaram, H.: Investigation of permeability alteration of fractured limestone reservoir due to geothermal heat extraction using three-dimensional thermo-hydro-chemical (THC) model, *Geothermics*, **51**, (2014), 46-62.

Pandey, S.N., Chaudhuri, A., Rajaram, H., and Kelkar, S.: Fracture transmissivity evolution due to silica dissolution/precipitation during geothermal heat extraction, *Geothermics*, **57**, (2015), 111-126.

Pasetto, D., Putti, M., and Yeh, W.W-G.: A Reduced-Order Model for Groundwater Flow Equation with Random Hydraulic Conductivity: Application to Monte Carlo methods, *Water Resources Research*, **49**, (2013), 3215-3228.

Pau, G.S.H., Zhang, Y., and Finsterle, S.: Reduced-Order Models for Many-Query Subsurface Flow Applications, *Computational Geosciences*, **17**, (2013), 705-721.

Qu, Q.-Z.: Model Order Reduction Techniques with Applications in Finite Element Analysis, *Springer*, (2004).

Quarteroni, A., and Rozza, G.: Reduced Order Methods for Modeling and Computational Reduction, *Modeling, Simulation & Applications Series*, Volume 9, *Springer*, (2014).

Robinson, B.A., and Tester, J.W.: Dispersed Fluid Flow in Fracture Reservoir: An Analysis of Tracer-Determined Residence Time Distributions, *Journal of Geophysical Research*, **89**, (1984), 10374-10384.

Rodrigues, N.E.V., Robinson, B.A., and Counce,D.A.: Tracer Experiment Results During the Long-Term Flow Test of the Fenton Hill Reservoir, *Proceedings*, 18th Stanford Geothermal Workshop, Stanford University, Stanford, CA, (1993).

Roff, A., Phillips, W.S., and Brown, D.W.: Joint Structures determined by Clustering Microearthquakes Using Waveform Amplitude Ratios, *International Journal for Rock Mechanics and Mining Sciences & Geomechanics Abstracts*, **25**, (1996), 627-639.

Schilders, W.H.A., vander Vorst, H.A., Rommes, J.: Model Order Reduction: Theory, Research Aspects, and Applications, Mathematics in Industry Series, Vol. 13, *Springer*, (2008).

Starfield, A.M., and Cundall, P.A.: Towards a Methodology for Rock Mechanics Modelling, *International Journal for Rock Mechanics and Mining Sciences & Geomechanics Abstracts*, **25**, (1988), 99-106.

Swenson, D., DuTeau, R., and Sprecker, T.: Modeling Flow in a Jointed Geothermal Reservoir, *Proceedings,* World Geothermal Congress, (1995).

White, M.D., and Philips, B.R.: Code Comparison Study Fosters Confidence in the Numerical Simulation of Enhanced Geothermal Systems, *Proceedings*, 40th Stanford Geothermal Workshop, Stanford University, Stanford, CA, (2016).

White, M.D., Elsworth, D., Sonnenthal, E., Fu, P., and Danko, G.: Challenge Problem Statements for a Code Comparison Study of Enhanced Geothermal Systems, *Proceedings*, 41st Stanford Geothermal Workshop, Stanford University, Stanford, CA, (2016).

White, S.K., Purohit, S., and Boyd, L.: Using GTO-Velo to Facilitate Communication and Sharing of Simultaneous Results in Support of the Geothermal Technologies Office Code Comparison Study, *Proceedings*, 41st Stanford Geothermal Workshop, Stanford University, Stanford, CA, (2016).

White, S.K., Kelkar, S.M., and Brown, D.W.: Bringing Fenton Hill into Digital Age: Data Conversion in Support of the Geothermal Technologies Office Code Comparison Study Challenge Problems, *Proceedings*, 41st Stanford Geothermal Workshop, Stanford University, Stanford, CA, (2016).